Published in final edited form as:
Birth Defects Res A Clin Mol Teratol. 2010 February ; 88(2): 111–127. doi:10.1002/bdra.20631.

Gene expression profiling in the fetal cardiac tissue after folate and low dose trichloroethylene exposure

Patricia T. Caldwell[1], **Ann Manziello**[3], **Jamie Howard**[1], **Brittany Palbykin**[1], **Raymond B. Runyan**[2,3], and **Ornella Selmin**[1,3]

[1]Department of Veterinary Science and Microbiology, University of Arizona, Tucson AZ.

[2]Cell Biology and Anatomy, University of Arizona, Tucson AZ.

[3]Southwest Environmental Health Sciences Center, University of Arizona, Tucson AZ.

Abstract

Background—Previous studies show gene expression alterations in rat embryo hearts and cell lines that correspond to the cardio-teratogenic effects of trichloroethylene (TCE) in animal models. One potential mechanism of TCE teratogenicity may be through altered regulation of calcium homeostatic genes with a corresponding inhibition of cardiac function. It has been suggested that TCE may interfere with the folic acid/methylation pathway in liver and kidney and alter gene regulation by epigenetic mechanisms. According to this hypothesis, folate supplementation in the maternal diet should counteract TCE effects on gene expression in the embryonic heart.

Approach—To identify transcriptional targets altered in the embryonic heart after exposure to TCE, and possible protective effects of folate, we used DNA microarray technology to profile gene expression in embryonic mouse hearts with maternal TCE exposure and dietary changes in maternal folate.

Results—Exposure to low doses of TCE (10ppb) caused extensive alterations in transcripts encoding proteins involved in transport, ion channel, transcription, differentiation, cytoskeleton, cell cycle and apoptosis. Exogenous folate did not offset the effects of TCE exposure on normal gene expression and both high and low levels of folate produced additional significant changes in gene expression.

Conclusions—A mechanism where TCE induces a folate deficiency does not explain altered gene expression patterns in the embryonic mouse heart. The data further suggest that use of folate supplementation, in the presence of this toxin, may be detrimental and non-protective of the developing embryo.

Keywords

Halogenated hydrocarbons; trichloroethylene; cardiac; folate; embryonic development; gene expression; ryanodine receptor

Corresponding Author: Ornella Selmin, PhD 1117 E. Lowell St., Building 90, Room CAF14 Department of Veterinary Science and Microbiology University of Arizona Tucson, AZ 85721-210090 selmin@u.arizona.edu Tel. 520-626-6087 Fax 520-621-6366.

1. Introduction

Halogenated hydrocarbons contaminate water supplies in the United States and around the world. Trichloroethylene (TCE) currently ranks 16th on the CERCLA Priority List of Hazardous Substances (ATSDR, 2007). It is generally used in industry as a degreasing agent and is found in paint removers, correction fluids, and household cleaners (Steinberg and DeSesso, 1993; Waters et al., 1977). Exposure to TCE through contaminated drinking water has been associated with increased incidence of congenital heart malformations in children born to exposed mothers and in model animals (Goldberg et al., 1990; Johnson et al., 1998b; Shaw et al., 1992; Spiegelstein et al., 2005).

TCE and Heart Development

The heart is the earliest functioning organ, first appearing as a simple linear tube that pumps in peristaltic fashion, and undergoing looping to form two chambers with the addition of primitive valves to inhibit retrograde flow (Forouhar et al., 2006; Liebling et al., 2006). The formation of the four chambered heart requires a series of septations in the atrioventricular canal, the atrium and the ventricle (Kirby, 2001). The first septation in the atrioventricular canal involves a process called epithelial-to-mesencyhmal transition (EMT) where endocardial cells migrate into the cardiac jelly, proliferate, and form valve leaflets (Armstrong and Bischoff, 2004). Proper developmental transitions are vital to heart function and embryo survival. Mutations in genes involved in these phases can lead to valve defects, disrupted blood flow and lethality (Clark et al., 2006; Joziasse et al., 2008).

Previous investigations using animal models have reported an association between TCE exposure and increased incidence of congenital heart malformations (Dawson et al., 1993; Goldberg et al., 1992; Johnson et al., 1998a; Johnson et al., 2003; Loeber et al., 1988;). More recently several groups have reported on possible mechanisms by which TCE may affect heart development. In the chick model, Boyer et al. (2000) demonstrated that exposure to 200ppb TCE reduced by 50% EMT of valve progenitors in a collagen gel assay, while lower doses of TCE in ovo enhanced valvuloseptal hypercellularity, endocardial cell proliferation and altered hemodynamic in the embryonic heart (Drake et al., 2006a; Drake et al., 2006b; Mishima et al., 2006). Others found that TCE exposure altered expression of the endothelial nitric oxide synthase and disrupted VEGF-stimulated endothelial proliferation in myocytes, suggesting a possible mechanism for TCE-mediated heart malformations (Ou et al., 2003). Our own studies indicated that exposure to TCE disrupted calcium flux regulation in myocytes (Caldwell et al., 2008). Heart morphogenesis is a complex process in which cascading events must be precisely orchestrated, so any external factor altering one or more of these events is likely to perturb normal cardiac development. Currently, there is no unifying hypothesis that reconciles the effects of TCE on the developing embryonic heart.

Folate and Heart Development

Epidemiological studies have shown maternal use of multivitamins in early pregnancy can reduce the risk for development of CHD in the fetus (Gelineau-van Waes et al., 2008). A study by Botto et al., (2003) showed that the risk of heart defects was lower in children born to mothers who used multivitamin supplements than in children of those who did not take

supplements. High levels of folate are usually included in recommended multivitamin supplements. Folate participates with vitamin B12 in the process that re-methylates homocysteine into methionine, which is the main methyl donor in form of S-adenosyl methionine (SAM) and is necessary for new synthesis of protein and nucleic acids. Folate is especially important in periods of rapid cell division and growth, as in infancy and pregnancy.

Chronic nutritional variations in folate metabolism may affect embryonic development and potentially increase incidence of cardiovascular defects because of the vital role of folate in DNA biosynthesis and amino acid metabolism (Li et al., 2005; Rosenquist et al., 1996). Only a few animal studies have been conducted on the effects of dietary folate and reproductive outcomes (Burgoon et al., 2002; Li et al., 2005; Sakanashi et al., 1996). A recent prevention trial in patients with prior colorectal polyps found an increased risk of reoccurrence when folic acid supplementation was used, suggesting a dual role of folate in carcinogenesis with potential support of tumor growth (Song et al., 2000).

It has been suggested that TCE induces folate deficiency in kidney by producing free radicals, which induce a B12 shortage, and consequently cause folate deficiency (Dow and Green, 2000). In rat, diet supplementation with methionine prevents the effects of TCE on induction of liver tumors, by reversing TCE-induced hypomethylation of c-myc and c-jun (Tao et al., 2000a; 2000b). To date, no studies have investigated whether trichloroethylene interferes with folate's metabolic pathways and, in turn, disrupts normal development of the embryo.

Previous work from our laboratory demonstrated that TCE exposure altered calcium regulation in cardiac myocytes and the expression of genes involved in calcium homeostasis (Caldwell et al., 2008; Selmin et al., 2008), suggesting a possible mechanism by which cardiac malformations occur. To identify other key contributing pathways that may be altered in the embryonic heart after exposure to TCE, we used DNA microarray technology to profile gene expression patterns in mice. Embryonic hearts were isolated from pregnant mice that had received a diet supplemented with low, normal, or high amounts of folate (0, 2, and 8mg/kg) in the presence or absence of 10ppb TCE in drinking water. The goal of this study was to measure transcriptional changes in the developing heart following exposure to low, environmentally significant doses of TCE, and to determine whether folic acid supplementation might counteract the effects of TCE. We found that high levels of folate supplementation with TCE exposure caused dramatic alterations in the expression level of genes involved in cellular pathways crucial for embryo development, such as transport, ion channels, differentiation, cytoskeleton, transcription, cell cycle and apoptosis. These findings suggest that a high folate diet does not offset low level TCE exposure and that the combination of TCE and high folate may have greater detrimental effects on development of the fetal heart.

2. Materials and Methods

All animals used in this study were maintained in a facility approved by the Association for Assessment and Accreditation of Laboratory Animal Care International and in accordance

with the established guidelines of the University of Arizona's Institutional Animal Care and Use Committee, the Animal Welfare Act, and U.S. Public Health Service policy standards.

2.1. Fetal Collection and Morphological Staging

Wild type mice (129S1/SvlmJ) were obtained from Jackson Laboratories (Bar Harbor, ME). Female mice were assigned to 3 different folate diets for four weeks before mating: 0mg/kg folate, 2mg/kg folate, and 8mg/kg folate (Dyets Version of the Clifford/Koury Folate Deficient L-Amino Acid Rodent Diet Without Succinyl Sulfathiazole, Modified for Pelleting; Dyets Inc, Bethlehem, PA), and received water *ad libitum*. The presence of a vaginal plug was considered indicative of day 0 pregnancy. At this time, each folate group was divided in two sub-groups of control and TCE exposed mice, and maternal exposure to 10ppbTCE was started via drinking water.

TCE was prepared daily in glass bottles that had been soaked in concentrated TCE solution overnight, rinsed and dried in a chemical hood before use. Each bottle was placed in metal casing to reduce light exposure and subsequent chemical breakdown. Control animals received distilled water throughout pregnancy.

At gestational time point of day 10, corresponding to the first phase of heart development, pregnant dams were sacrificed by CO2 inhalation, the abdomen opened and the uterine contents removed. The location of all viable fetuses and reabsorption sites were recorded. Decidual capsules were transferred to a phosphate-buffered saline solution and embryos were dissected free. All embryos were examined grossly for size and developmental stage. Cardiac tissue was removed from each viable embryo and placed in RNA later for future use. Maternal organs were also harvested for additional studies. Whole fetuses were viewed under a Nikon SMZ-2T stereomicroscope.

2.2. RNA extraction

Total RNA was extracted from pooled embryo hearts (n= 35, corresponding to 4-6 litters) and purified using a custom RNA extraction method. Briefly, the RNAlater solution was removed from the merged heart pools. 100uL RLT buffer with 1% B-mercaptoethanol and 600ul Trizol (Invitrogen, Carlsbad, CA) was added and mixed. RNA extraction was performed according to manufacturer instructions. Dry RNA pellets were resolubilized in 30uL RNAase-free dionized water. RNeasy Mini Kits (Qiagen, Valencia, CA) were used for further RNA cleanup if needed.

2.3. RNA and microarray preparation

Six sample groups (control and TCE exposed from each one of the three folate diet groups) were tested, each with two biological replicates for a total of 12 sample groups. Total RNA from each group was processed by the University of Arizona microarray facility (Genomics Shared Service, Tucson, AZ). RNA purity was evaluated using an Eppendorf BioPhotometer (Eppendorf North America, Westbury, NY) to obtain values of nucleotides, organics, proteins, and contaminants in the samples. Viable RNA had 260/280 ratios between 1.8 and 2.0 or higher. RNA integrity was confirmed using an Agilent 2100 Bioanalyzer (Agilent Technologies, Waldbronn, Germany) following the RNA 6000 Nano Chip Series II Assay

protocol. Twelve Affymetrix Mouse Gene 1.0 ST arrays (Affymetrix, Santa Clara, CA) containing over 28,000 gene-level probe sets were used for genome wide expression profiling. The arrays were processed according to the protocol (GeneChip Whole Transcript) Sense Target Labeling Assay Manual, version4) established by Affymetrix. Briefly, 400ng of total RNA were reverse transcribed into double stranded cDNA using the Affymetrix WT cDNA Synthesis and Amplification kit. The entire cDNA was then transcribed into cRNA overnight, cleaned using the Affymetrix GeneChip Sample Cleanup Module, and quantified on a NanoDrop 1000 (Thermo Scientific, Wilmington, DE). 8ug of cRNA were reverse transcribed into ssDNA, and labeled. Aliquots of the labeled DNA were combined with the hybridization solution overnight. The arrays were scanned using the Affymetrix GeneChip Scanner 3000 with 7G upgrade. The image generated was analyzed using the Affymetrix GeneChip Operating Software (GCOS) were .DAT (image), .CEL (cell intensity data), .CHP (probe analysis data) files were generated.

2.4. Statistical analysis of DNA microarrays

The Affymetrix mouse gene ST arrays were processed with a bioconductor library (http://www.bioconductor.org) designed for this array. The arrays were then normalized using the RMA function in the oligo library of bioconductor. In order to identify poor quality arrays, Spearman correlation coefficients between all arrays were computed. A plot of the coefficients revealed that correlations between all arrays were 0.98 or greater, indicating that a relatively small number of genes were changing in response to the treatments. As a further control, the distribution of values for positive and negative control probes were examined on each array and were found to have the correct expected separation. The samples included 2 arrays representing two biological replicates for each treatment.

Since there were only two replicates due to the complexity of the sample preparation, a specific approach was used that identified probes that showed a consistent change between biological duplicates. A cutoff value for the change between treatments of 1.5 fold was chosen based on an examination of the distribution of expression values on these arrays and identified approximately 200-1000 probes that were varying to the greatest extent. Probe lists were generated as described below.

Briefly, the objective was to find genes that were changing between treatments while reducing the effects of the biological variation between duplicate samples. To compare two treatments, probe expression ratios for all 4 possible combinations of the duplicate arrays were calculated. If 2 or more of these ratios were 1.5 fold or greater, the gene was considered to be changed. These probe sets were annotated using Affymetrix data files and the affected genes, biological functions, and pathways were identified. For the biochemical pathway analysis, lists of genes involved in pathways of biological interest were obtained from the KEGG database using the BIORAG resource (http://www.biorag.org). Genes showing expression ratios between treatments of greater than 1.5 fold were then identified.

2.5. Reverse-transcriptase and quantitative real-time PCR

Total RNA from pooled embryos was transcribed into cDNA using the ISCRIPT cDNA synthesis kit (Bio-Rad Laboratories, Hercules, CA). Gene specific primers were used to

amplify mouse β-actin, Ryr2, ErbB, Sumo1, INSR, GATA3, Cubn, and Gstp2 transcripts. Primers for the six transcripts and the housekeeping gene were designed using the NCBI Primer-BLAST program. SYBR Green analysis using ITAQ SYBR Green supermix with ROX (Bio-rad Laboratories, Hercules, CA) was used according to the manufacturer's instructions and carried out using the gene specific primers to ensure that single band dissociation was acquired. Briefly, the real-time PCR reactions were run at a final volume of 25 μL consisting of the following master mix: 12.5 μL of 10× buffer supermix, 1 μL each of forward and reverse primers (10μM), 9.5 μL nuclease free double-distilled water, and 1μL cDNA (1μg/μl). The ABI 7300 Real Time PCR System and Ct values were used to quantify the relative differences in PCR product. Each sample was run a minimum of three times in duplicate using the same two pools of RNA used for the microarray analysis. Expression values for each specific gene were normalized against β-actin expression levels, and expressed in fold change. Values represent means +/− standard deviation (SD). SD was calculated as the ratio of SD of the sample pool (n = or > 6) divided by the average of n.

3. Results

3.1. Physical outcomes of Day 10 embryos

We performed a gross examination of each embryo after removal from the dam, and recorded the results in Table 2. Any empty amniotic sac was recorded as reabsorption. If no amniotic sacs were found in the womb, it was considered false pregnancy. Developmental stages were determined using mouse embryonic development charts (Kaufman, 1992) (Figure 1D). For each category, the first number represents a “per litter basis” of change, the second one is the percent change based on total number of embryos used in each group.

Examining the different levels of folate diet alone, without TCE exposure, both 0mg/kg (0CTL) and 8mg/kg (8CTL) folate increased the number of reabsorptions and under-developed embryos compared with the control group (2mg/kg folate, 2CTL). Normally developed embryos were reduced by 10% or more in 0CTL and 8CTL respectively, when compared against 2CTL. In the 10ppb TCE exposed embryo populations, these finding were inverted. We observed that the number of reabsorptions was decreased by ~5% in the 2mg/kg (2TCE) and 8mg/kg (8TCE) folate groups when compared against the non-exposed, control group, 2CTL. Interestingly, the percentage of reabsorptions in the 0T embryos was identical (21.3%) to 2CTL. When 0TCE and 8TCE were compared to 2TCE, we observed an increased number of reabsorptions with both low and high levels of folate in the maternal diet. In addition, there were between 7-10% less underdeveloped embryos, and 2-4% more normally developed embryos with high and low folate, respectively. Finally, the rate of false pregnancy did not change considerably across the different groups. The 0TCE and 2CTL groups had the same percentage of normally developed embryos.

3.2. Microarray Results

We used Venn diagrams to represent possible relations between comparison data sets (Figure 2). The numbers in the circle represents genes changed uniquely in a particular group and the overlapping sections show the number of altered genes in common between two, or all three groups. Figure 2A shows comparisons between 2CTL against all three

folate levels in the presence of 10ppb TCE (0TCE, 2TCE, and 8TCE), separated into over and under-expressed transcripts. This comparison illustrates how TCE exposure in deficient, normal, and high folate groups altered transcript levels when compared to the non-exposed group at a normal folate level. Taking together the over and under-expressed diagrams, we observed that the most genes changed in the 8TCE group (2CTL v 8TCE) (3340 total), whereas 2894 transcripts were altered in 0TCE and 1226 in 2TCE. Furthermore, the overlap between 8TCE and 0TCE showed the highest number of similarly changed genes. Interestingly, all numbers in the under-expressed diagrams are much higher than in the over-expressed diagrams.

We also compared TCE exposed versus non-exposed (CTL) groups at each of the three folate levels (Figure 2B). This diagram illustrates how TCE exposure in deficient, normal, and high folate diets altered transcript expression when compared against similar folate controls. Both over and under-expressed diagrams show a striking number of genes altered in 8TCE versus 8CTL group (1555 and 1484, respectively). 2TCE versus 2CTL is the next highest, totaling 861 under-expressed genes. In both over and under-expressed diagrams fewer than 10 genes were similarly altered by all three groups.

3.3. Gene expression changes in cellular pathways

In order to better define the effects of TCE on gene expression at different levels of folate, we grouped the down- and up- regulated transcripts based on their involvement in specific cellular pathways, and then compared each group as illustrated in Figure 3. In the first three columns, TCE exposed embryos at deficient, normal, and high folate levels were compared against their own non-exposed group. Columns 4 and 5 compared 0TCE and 8TCE against the 2TCE group. These two columns illustrate the different contribution of TCE to transcriptional change in combination with different folate levels. Columns 6 and 7 compared OCTL and 8CTL against 2CTL. These columns display the effects of different levels of folate alone on gene expression.

In column 1, 0CTL v OTCE shows 107 altered transcripts representing less than 0.4% of all genes on the microarrays, with the majority involved in the transport pathway. In column 2, 2CTL v 2TCE displays 252 transcripts, corresponding to less than 0.9% of all genes represented. In particular, the majority of these changes occurred in the transcription (56 altered transcripts) and transport (61 altered transcripts) pathways. In column 3, 8CTL v 8TCE shows the most dramatic alterations, with changes in over 3% of the total transcripts: Between 20 and 30 genes were altered in the calcium, DNA repair, extra-cellular matrix, immune system, and ion channels pathways; between 30 and 60 gene changes were observed in the adhesion, apoptosis, cell cycle, cytoskeleton, and differentiation pathways, while 209 genes were altered in both transcription and transport pathways.

In columns 4 and 5, we compared the expression levels in 0TCE and 8TCE against the 2TCE group. In column 4, the adhesion, apoptosis, calcium, extra-cellular matrix, cytoskeleton, and differentiation pathways all revealed between 10 and 30 altered transcripts. The most robust alterations occurred in the transcription (48 under-expressed), and transport pathways (32 over- and 67 under-expressed). In column 5, the number of transcripts altered in 2TCE v 8TCE is lower than the number in column 3, where we

compared 8CTL v 8TCE. The decrease was more pronounced in the transcription, apoptosis, cell cycle, cytoskeleton (~50%), and differentiation and transport pathway (32 and 21% fewer genes, respectively).

In columns 6 and 7, expression levels in 0CTL and 8CTL were compared to 2CTL and showed the most pronounced changes, indicating a drastic effect of folate level on gene expression. At low folate level (column 6), over 50 transcripts were altered in the apoptosis and cytoskeleton pathways, and over 70 in the differentiation pathway. At high folate level (column 7), over 80 transcripts were altered in the differentiation, over 60 in the adhesion, apoptosis and cell cycle, and over 50 in the cytoskeleton pathways.

3.4. TCE effects on individual pathways

Upon examination of individual pathways, we observed common themes of expression changes across some of the comparison columns, in particular, in the calcium and ion channel pathways. The majority of over-expressed genes in the 8CTLv 8TCE and 2CTL v 8TCE groups (Table 3A, 4A: columns 3 and 5) were actually under-expressed in 2CTL v 0CTL and 2CTL v 8CTL (Table 3B, 4B: columns 6 and 7). In both pathways we observed expression changes in genes coding for calcium, potassium, sodium and voltage-gated channels, including Ryr2, NCX, Mef2, and ErbB4. The apoptosis and cell cycle pathways (Tables 5 and 6) show the majority of changes occurring in 8CTL v 8TCE, with 30-40 transcript alterations in both the over and under-expressed tables, 15% of these with over 2-fold changes. In both 2CTL v 0CTL, and 2C TL v 8CTL (Columns 6 and 7) over 40 transcripts were under-expressed. 0CTL v 0TCE and 2CTL v 2TCE (Column 1 and 2) show minor alterations in both pathways with 5 or less genes except for 11 under-expressed genes in the 2CTL v 2TCE group.

3.5. Real-time analysis of expression changes of selected genes

We selected eight transcripts that were altered by TCE in either 8CTL v 8TCE or 0CTL v 0TCE groups, and measured their expression levels by real-time PCR. The objective was to confirm the findings of the microarray analysis by a more sensitive technique. We chose to analyze two genes involved in calcium signaling (Ryr2 and NCX), and two genes involved in cellular growth (INSR and ERBB4). Gata3 was selected for its role during cardiomyocyte differentiation and early steps of heart tube morphogenesis (Cripps and Olson, 2002), and Glutathione-S-Transferase (GstP) for its importance in detoxification pathways. We selected the receptor Cubilin (gp280) (Sahali et al., 1988; Smith et al., 2006) and Sumo1, encoding for a protein that mediates sumoylation of histones and transcription factors, for their role in regulation of transcription during embryogenesis (Alkuraya et al., 2006).

Overall, the results obtained with real-time PCR are consistent with those from the microarray analysis. Figure 4A confirmed up-regulation of INSR, NCX, ERBB4, RYR2, and Gata3 in the 8TCE group. Sumo1 and Cubilin were found under-expressed in the microarray analysis, but no significant regulation was observed by real-time PCR. In 0TCE, the expression change in the three genes tested (Figure 4B) were similar to those in the microarray, although the difference was not significant for Cubilin and Gstp.

4. Discussion

4.1. Physical outcomes of Day 10 embryos

The results from Table 2 suggest two conclusions: 1) Both high and low folate in the maternal diet leads to similar phenotypic outcomes in the embryos; and 2) Exposure to 10ppb TCE counteracted the effects of high and low folate alone. In both 0CTL and 8CTL, we observed an increased rate of reabsorbed and developmentally delayed embryos, and a decrease in normally developed embryos. However, when compared to 0TCE and 8TCE, we observed an almost perfect inversion of phenotypic outcomes (Table 2). Folate is a critical player in pathways involved in amino acid metabolism, nucleotide synthesis and methylation reactions (Wagner, 1995) so it is possible that any variation from a physiological optimum level of folate may create disturbances in one or more of these pathways. This hypothesis is corroborated by the finding that in 0TCE we observed no change in the percentage of reabsorptions and normally developed embryos when compared to 2CTL. Overall, these results suggest that TCE may facilitate the progression of these embryos through otherwise restrictive developmental checkpoints. A detailed examination of embryos is necessary to identify number and type of heart defects possibly present in each group, however, this aim will have to be addressed in future experiments.

4.2. Gene expression changes in cellular pathways

An expected finding of this study is that many changes in gene expression occurred in embryonic hearts in the 0CTL and 8CTL groups, underlying the importance of folate for development. However, TCE exposure in the presence of high folate induced the highest number of changes. This observation suggests that the effects of TCE are more dramatic and potentially detrimental to cardiac development in the presence of high folate levels in the maternal diet.

Calcium signaling is a crucial pathway for heart function (Table 3), and these findings corroborate those previously reported by our group, using in vitro models (Caldwell et al., 2008; Selmin et al., 2008). It is notable that only three out of 414 genes were altered in the 2CTL v 2TCE group and absolutely no changes were observed in the 0CTL v 0TCE level. This finding supports that notion that no further damage is caused by TCE exposure in an environment already under substantial stress due to deficient folate levels.

Ion channels are integral membrane proteins that regulate the flow of ions across the membrane and are fundamental to maintaining proper ion concentrations inside the cell (Table 4). Our data show that high folate levels in combination with TCE exposure induced over-expression of many genes in the ion channel pathway. The majority of the over-expressed genes encodes for potassium, calcium, and other cation transportation channels and corroborates previously published data from our laboratory (Caldwell et al., 2008) showing an increased calcium flux from the sarcoplasmic reticulum in cardiomyocytes exposed to 10ppb TCE. Our microarray data may be explained by TCE ability to interfere with potassium and calcium channels. Since calcium and potassium ions are very similar (both having positive charges, similar electron orbitals and atomic weights) TCE may alter the binding affinity of both channels or maintain the channels open to create a type of super-

highway for calcium transport. Alternatively, TCE could alter the permeability of the cell membrane, causing an electrolyte imbalance and thus activating signaling pathways that increase synthesis of ion channels to correct the imbalance.

Significant alterations in gene expression were observed in the apoptosis and cell cycle pathways (Tables 5 and 6). Apoptosis is essential for the development of organs and structures throughout the embryonic stages, and is closely interconnected with pathways mediating the signals that direct the cell through the different phases of DNA synthesis, repair, and mitosis. Past studies have linked TCE exposure to septal and valvular malformations, hypercellularity and endocardiocyte proliferation (Drake et al., 2006a; Drake et al., 2006b; Hoffmann et al., 1994). Our results indicate that high levels of folate reduced cell cycle and apoptotic signals overall, but in the presence of 10ppb TCE, many of these signals were reversed, providing a possible explanation for the cardiac hypercellularity and induced proliferation observed by other groups.

4.3. Overall conclusions

Epidemiological and animal studies have documented the dual effect of folate on carcinogenesis: protecting normal mucosa, but enhancing progression of early lesions (Kim, 2004). Taken together, our findings also suggest that folate may have a dual effect on cardiogenesis, depending on the presence of environmental toxins, such as TCE. Additionally, our data support the notion that environmental concentrations of TCE may cause drastic changes in gene expression during critical phases of heart development. Notwithstanding the limitations associated with our study, these data suggest that the optimal dose of folate intervention needs to be determined for safe and effective prenatal care. The data also indicate that exogenous folate, whether to restore normal folate levels or raise endogenous levels does not strongly offset the effects of TCE exposure on altered gene expression. Thus, a mechanism where TCE produces a folate deficiency does not explain altered gene expression patterns in the embryonic mouse heart.

Acknowledgments

We thank the Genomics Facility Core, especially Candace Clark and Jose Munoz-Rodriguez, and the Bioinformatics Service, especially David Mount, of the Southwest Environmental Health Sciences Center and Arizona Cancer Center at the University of Arizona for carrying out the microarray hybridization and data analysis. Thanks to P.A. Thorne and David Perkins for their technical assistance.

This work was supported by NIH, SBPR Program No P42ES04940 (O.S and R.R), and by NIH, NIEHS Grant No. ES06694 (SWEHSC)

References

Alkuraya FS, Saadi I, Lund JJ, Turbe-Doan A, Morton CC, Maas RL. SUMO1 haploinsufficiency leads to cleft lip and palate. Science. 2006; 313(5794):1751. [PubMed: 16990542]

Armstrong EJ, Bischoff J. Heart valve development: endothelial cell signaling and differentiation. Circ Res. 2004; 95(5):459–470. [PubMed: 15345668]

ATSDR- Agency for Toxic Substances and Disease Registry. 2007 CERCLA Priority List of Hazardous Substances. Department of Health and Human Services; Atlanta: 2007.

Botto LD, Mulinare J, Erickson JD. Do multivitamin or folic acid supplements reduce the risk for congenital heart defects? Evidence and gaps. Am J Med Genet A. 2003; 121(2):95–101.

Boyer AS, Finch WT, Runyan RB. Trichloroethylene inhibits development of embryonic heart valve precursors in vitro. Toxicol Sci. 2000; 53(1):109–117. [PubMed: 10653528]

Burgoon JM, Selhub J, Nadeau M, Sadler TW. Investigation of the effects of folate deficiency on embryonic development through the establishment of a folate deficient mouse model. Teratology. 2002; 65(5):219–227. [PubMed: 11967921]

Caldwell PT, Thorne PA, Johnson PD, Boitano S, Runyan RB, Selmin O. Trichloroethylene disrupts cardiac gene expression and calcium homeostasis in rat myocytes. Toxicol Sci. 2008; 104(1):135–143. [PubMed: 18411232]

Clark KL, Yutzey KE, Benson DW. Transcription factors and congenital heart defects. Annu Rev Physiol. 2006; 68:97–121. [PubMed: 16460268]

Cripps RM, Olson EN. Control of cardiac development by an evolutionarily conserved transcriptional network. Dev Biol. 2002; 246(1):14–28. [PubMed: 12027431]

Dawson BV, Johnson PD, Goldberg SJ, Ulreich JB. Cardiac teratogenesis of halogenated hydrocarbon-contaminated drinking water. J Am Coll Cardiol. 1993; 21(6):1466–1472. [PubMed: 8473657]

Dow JL, Green T. Trichloroethylene induced vitamin B(12) and folate deficiency leads to increased formic acid excretion in the rat. Toxicology. 2000; 146(2-3):123–136. [PubMed: 10814845]

Drake VJ, Koprowski SL, Hu N, Smith SM, Lough J. Cardiogenic effects of trichloroethylene and trichloroacetic acid following exposure during heart specification of avian development. Toxicol Sci. 2006a; 94(1):153–162. [PubMed: 16917067]

Drake VJ, Koprowski SL, Lough JW, Smith SM. Gastrulating chick embryo as a model for evaluating teratogenicity: a comparison of three approaches. Birth Defects Res A Clin Mol Teratol. 2006b; 76(1):66–71. [PubMed: 16333841]

Forouhar AS, Liebling M, Hickerson A, Nasiraei-Moghaddam A, Tsai HJ, Hove JR, Fraser SE, Dickinson ME, Gharib M. The embryonic vertebrate heart tube is a dynamic suction pump. Science. 2006; 312(5774):751–753. [PubMed: 16675702]

Gelineau-van Waes J, Heller S, Bauer LK, Wilberding J, Maddox JR, Aleman F, Rosenquist TH, Finnell RH. Embryonic development in the reduced folate carrier knockout mouse is modulated by maternal folate supplementation. Birth Defects Res A Clin Mol Teratol. 2008; 82(7):494–507. [PubMed: 18383508]

Goldberg SJ, Dawson BV, Johnson PD, Hoyme HE, Ulreich JB. Cardiac teratogenicity of dichloroethylene in a chick model. Pediatr Res. 1992; 32(1):23–26. [PubMed: 1635841]

Goldberg SJ, Lebowitz MD, Graver EJ, Hicks S. An association of human congenital cardiac malformations and drinking water contaminants. J Am Coll Cardiol. 1990; 16(1):155–164. [PubMed: 2358589]

Hoffmann P, Heinroth K, Richards D, Plews P, Toraason M. Depression of calcium dynamics in cardiac myocytes--a common mechanism of halogenated hydrocarbon anesthetics and solvents. J Mol Cell Cardiol. 1994; 26(5):579–589. [PubMed: 8072012]

Johnson PD, Dawson BV, Goldberg SJ. Cardiac teratogenicity of trichloroethylene metabolites. J Am Coll Cardiol. 1998a; 32(2):540–545. [PubMed: 9708489]

Johnson PD, Dawson BV, Goldberg SJ. A review: trichloroethylene metabolites: potential cardiac teratogens. Environ Health Perspect. 1998b; 106(Suppl 4):995–999. [PubMed: 9703484]

Johnson PD, Goldberg SJ, Mays MZ, Dawson BV. Threshold of trichloroethylene contamination in maternal drinking waters affecting fetal heart development in the rat. Environ Health Perspect. 2003; 111(3):289–292. [PubMed: 12611656]

Joziasse IC, van de Smagt JJ, Smith K, Bakkers J, Sieswerda GJ, Mulder BJ, Doevendans PA. Genes in congenital heart disease: atrioventricular valve formation. Basic Res Cardiol. 2008; 103(3):216–227. [PubMed: 18392768]

Kaufman, MH. The Atlas of the Mouse Development. Academic Press; London: 1992.

Kim YI. Folate, colorectal carcinogenesis, and DNA methylation: lessons from animal studies. Environ Mol Mutagen. 2004; 44(1):10–25. [PubMed: 15199543]

Kirby M. Getting to the heart of cardiac morphogenesis. Circ Res. 2001; (88):370–372. [PubMed: 11230101]

Li D, Pickell L, Liu Y, Wu Q, Cohn JS, Rozen R. Maternal methylenetetrahydrofolate reductase deficiency and low dietary folate lead to adverse reproductive outcomes and congenital heart defects in mice. Am J Clin Nutr. 2005; 82(1):188–195. [PubMed: 16002818]

Liebling M, Forouhar AS, Wolleschensky R, Zimmermann B, Ankerhold R, Fraser SE, Gharib M, Dickinson ME. Rapid three-dimensional imaging and analysis of the beating embryonic heart reveals functional changes during development. Dev Dyn. 2006; 235(11):2940–2948. [PubMed: 16921497]

Loeber CP, Hendrix MJ, Diez De Pinos S, Goldberg SJ. Trichloroethylene: a cardiac teratogen in developing chick embryos. Pediatr Res. 1988; 24(6):740–744. [PubMed: 3205631]

Mishima N, Hoffman S, Hill EG, Krug EL. Chick embryos exposed to trichloroethylene in an ex ovo culture model show selective defects in early endocardial cushion tissue formation. Birth Defects Res A Clin Mol Teratol. 2006; 76(7):517–527. [PubMed: 16933305]

Ou J, Ou Z, McCarver DG, Hines RN, Oldham KT, Ackerman AW, Pritchard KA Jr. Trichloroethylene decreases heat shock protein 90 interactions with endothelial nitric oxide synthase: implications for endothelial cell proliferation. Toxicol Sci. 2003; 73(1):90–97. [PubMed: 12657742]

Rosenquist TH, Ratashak SA, Selhub J. Homocysteine induces congenital defects of the heart and neural tube: effect of folic acid. Proc Natl Acad Sci U S A. 1996; 93(26):15227–15232. [PubMed: 8986792]

Sahali D, Mulliez N, Chatelet F, Dupuis R, Ronco P, Verroust P. Characterization of a 280-kD protein restricted to the coated pits of the renal brush border and the epithelial cells of the yolk sac. Teratogenic effect of the specific monoclonal antibodies. J Exp Med. 1988; 167(1):213–218. [PubMed: 2891781]

Sakanashi TM, Rogers JM, Fu SS, Connelly LE, Keen CL. Influence of maternal folate status on the developmental toxicity of methanol in the CD-1 mouse. Teratology. 1996; 54(4):198–206. [PubMed: 9122889]

Selmin OI, Thorne PA, Caldwell PT, Taylor MR. Trichloroethylene and trichloroacetic acid regulate calcium signaling pathways in murine embryonal carcinoma cells p19. Cardiovasc Toxicol. 2008; 8(2):47–56. [PubMed: 18437584]

Shaw GM, Schulman J, Frisch JD, Cummins SK, Harris JA. Congenital malformations and birthweight in areas with potential environmental contamination. Arch Environ Health. 1992; 47(2):147–154. [PubMed: 1567240]

Smith BT, Mussell JC, Fleming PA, Barth JL, Spyropoulos DD, Cooley MA, Drake CJ, Argraves WS. Targeted disruption of cubilin reveals essential developmental roles in the structure and function of endoderm and in somite formation. BMC Dev Biol. 2006; 6:30. [PubMed: 16787536]

Song J, Medline A, Mason JB, Gallinger S, Kim YI. Effects of dietary folate on intestinal tumorigenesis in the apcMin mouse. Cancer Res. 2000; 60(19):5434–5440. [PubMed: 11034085]

Spiegelstein O, Gould A, Wlodarczyk B, Tsie M, Lu X, Le C, Troen A, Selhub J, Piedrahita JA, Salbaum JM, Kappen C, Melnyk S, James J, Finnell RH. Developmental consequences of in utero sodium arsenate exposure in mice with folate transport deficiencies. Toxicol Appl Pharmacol. 2005; 203(1):18–26. [PubMed: 15694460]

Steinberg AD, DeSesso JM. Have animal data been used inappropriately to estimate risks to humans from environmental trichloroethylene? Regul Toxicol Pharmacol. 1993; 18(2):137–153. [PubMed: 8278637]

Tao L, Yang S, Xie M, Kramer PM, Pereira MA. Effect of trichloroethylene and its metabolites, dichloroacetic acid and trichloroacetic acid, on the methylation and expression of c-Jun and c-Myc protooncogenes in mouse liver: prevention by methionine. Toxicol Sci. 2000a; 54(2):399–407. [PubMed: 10774822]

Tao L, Yang S, Xie M, Kramer PM, Pereira MA. Hypomethylation and overexpression of c-jun and c-myc protooncogenes and increased DNA methyltransferase activity in dichloroacetic and trichloroacetic acid-promoted mouse liver tumors. Cancer Lett. 2000b; 158(2):185–193. [PubMed: 10960769]

Wagner C. Biochemical role of folate in cellular metabolism. Folate in Health and Disease. 1995:23–42.

Waters EM, Gerstner HB, Huff JE. Trichloroethylene. I. An overview. J Toxicol Environ Health. 1977; 2(3):671–707. [PubMed: 403297]

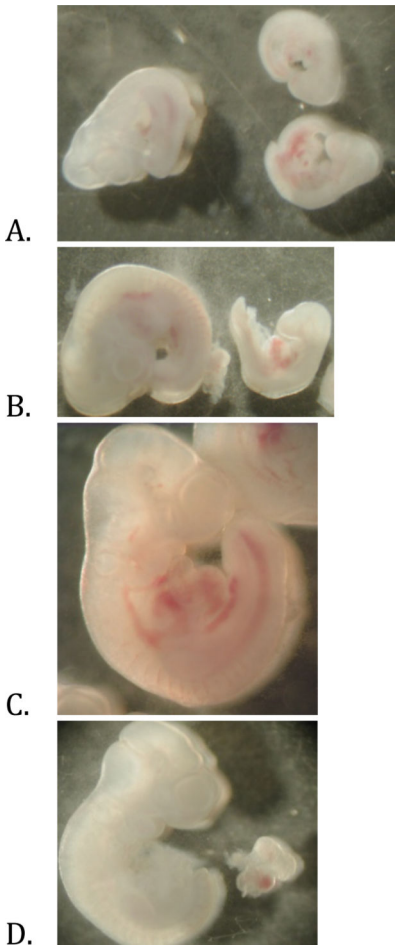

Figure 1. Developmental phenotype of Day 10 embryos

A) Littermates from non-exposed dam on 0mg/kg folate. Day10 embryo shown on left with two under-developed embryos shown on right. B) Embryos from non-exposed dam on 8mg/kg folate. Day 10 embryo on left with under-developed embryo on right. C) Embryo from 10ppb TCE exposed dam on 0mg/kg folate. D) Day 10 embryo from control 2mg/kg folate group with cardiac tissue removed.

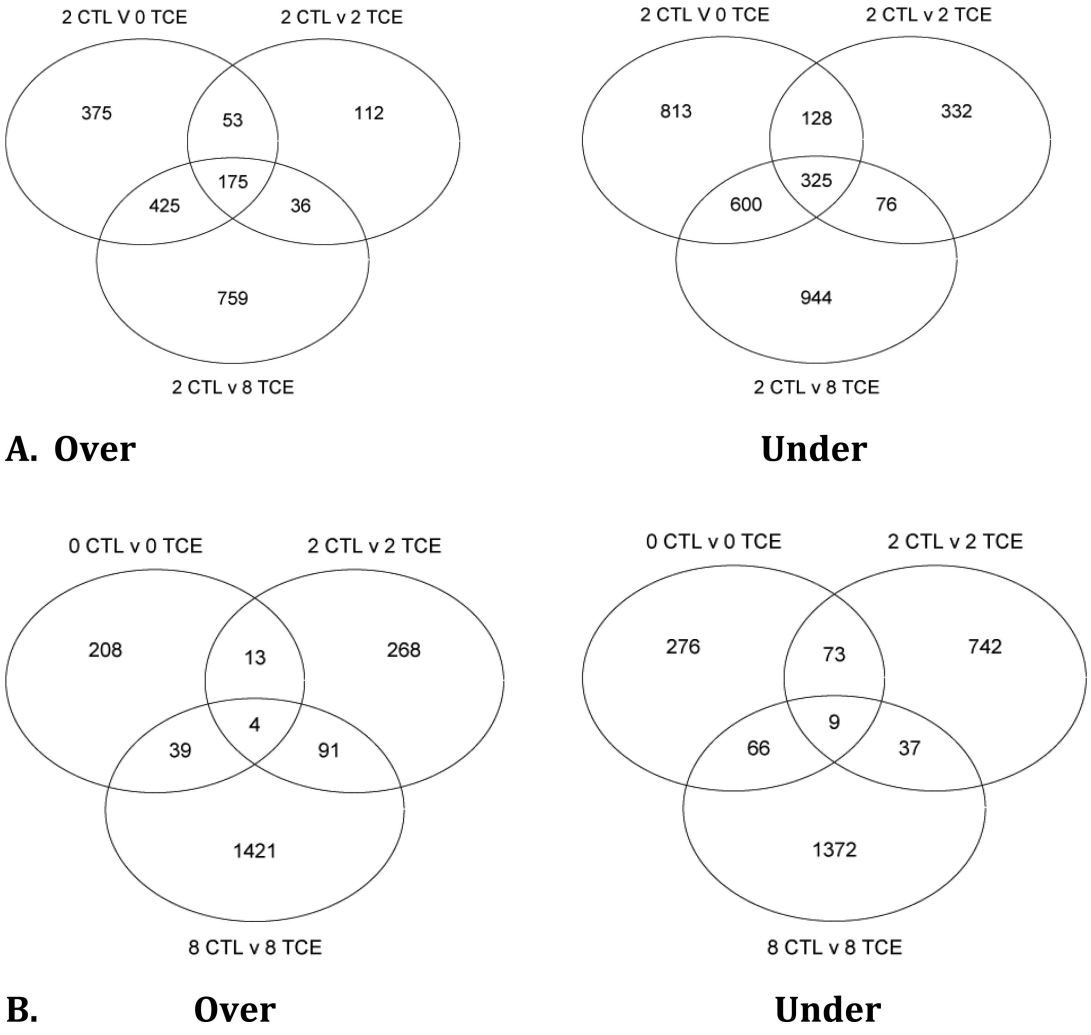

Figure 2. Venn Diagrams

Overview of all genes altered in day 10 embryonic cardiac tissue microarrays. A) Shows comparisons between the 2mg/kg control group (2CTL) against all TCE-treated groups (OTCE, 2TCE, 8TCE). 2CTL v 0 (2, or 8) TCE include transcripts that were either under or over expressed in the TCE groups when compared with the control, 2CTL group. B) Shows comparisons between each individual TCE exposed group (OTCE, 2TCE, 8TCE) against their own folate level control group (OCTL, 2CTL, 8C).

	1		2		3		4		5		6		7	
Pathway	0 CTL v 0 TCE		2 CTL v 2 TCE		8 CTL v 8 TCE		2 TCE v 0 TCE		2 TCE v 8 TCE		2 CTL v 0 CTL		2 CTL v 8 CTL	
	over	under	over	under	over	under	over	under	over	under	over	under	over	under
Adhesion	0	5	6	16	29	11	16	10	39	4	31	31	23	40
Apoptosis	4	5	5	11	34	39	4	26	18	18	13	63	21	48
calcium	0	0	0	3	18	3	5	10	7	6	5	23	3	27
cell cycle	2	0	7	3	30	34	11	18	9	21	16	43	16	44
DNA repair	2	0	2	1	14	9	1	4	1	6	2	10	5	16
ECM	0	3	3	4	23	7	15	7	22	4	18	9	13	18
immune	1	1	3	12	27	6	5	1	28	3	11	11	7	9
insulin	0	2	2	0	11	5	0	4	2	3	2	11	2	12
Ion Channel	0	2	0	10	14	1	4	3	11	1	9	17	3	23
Lipids	0	0	0	1	4	6	1	4	5	8	3	12	2	8
Methionine	2	1	2	1	6	7	1	5	1	11	5	16	5	18
Traffic	0	0	0	0	1	2	0	0	0	2	0	1	1	4
Transcription	8	9	27	28	118	80	15	48	44	57	59	140	54	146
Translation	4	0	2	2	7	8	2	6	3	2	3	13	5	4
Transport	8	30	23	38	77	127	32	67	72	91	76	180	57	179
Cytoskeleton	3	4	1	12	30	21	5	13	11	13	7	58	7	52
Differentiation	3	7	12	14	46	30	14	18	34	18	30	69	26	55
Glyco Metabolism	0	1	1	0	2	7	0	4	0	5	2	12	2	8

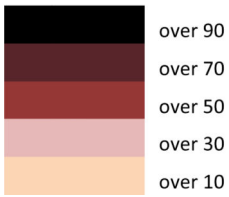

Figure 3. Overall gene expression changes

Numbers in each box represent genes over- or under-expressed in each one of the six comparison group, and assigned to specific Kegg pathways. In the first 3 columns, expression level of transcripts in the TCE exposed embryos at low, normal, and high folate were compared against non-exposed embryos at the same folate level. Columns four and five evaluate changes in the TCE exposed embryos at 0 and 8mg/kg folate level compared against the 2mg/kg folate level exposed to 10ppb TCE. Columns six and seven indicate the number of transcripts altered in the 0 and 8mg/kg folate controls compared against 2mg/kg folate control embryos, therefore account for folate-induced changes only.

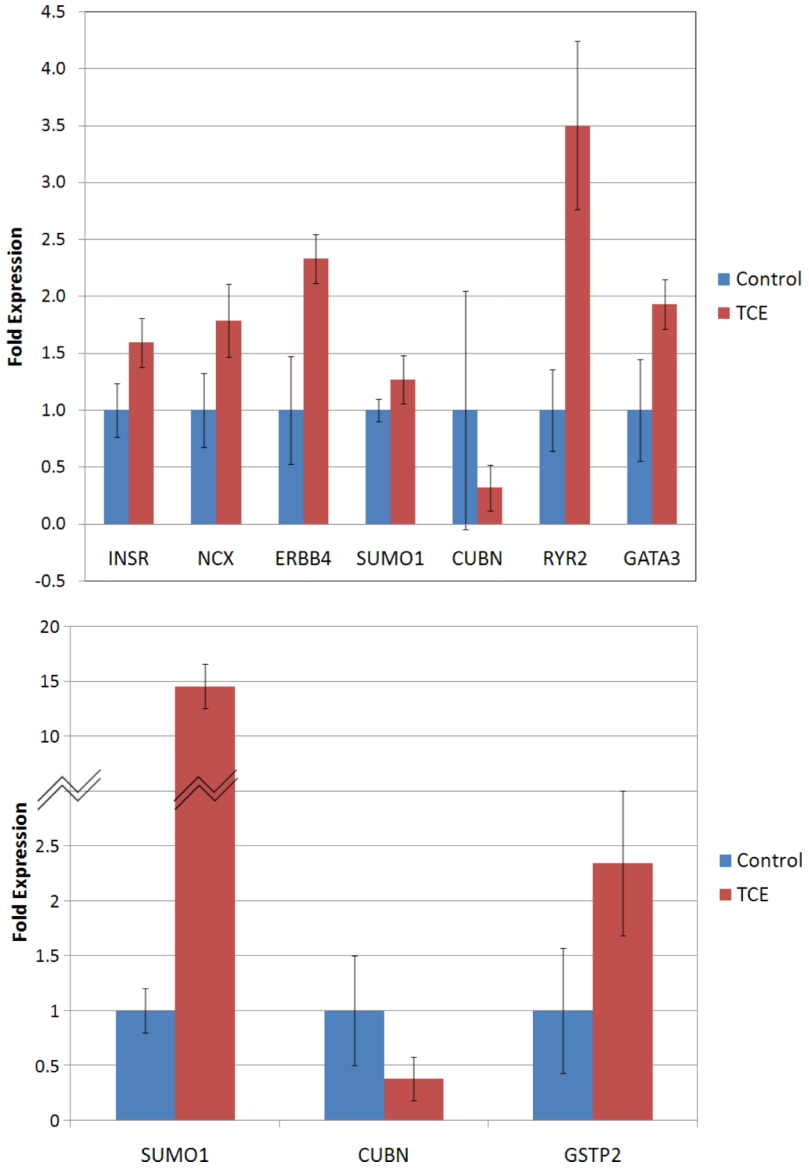

Figure 4. Real-time PCR analysis of transcripts selected for microarray validation

Aliquots of RNA from the same two biological RNA pools used in the microarray analysis were run in duplicates at least three different times. Bars represent average values between different runs +/- SD.

Table 1

Sequences of the primers used for realtime PCR

Gene	GenBank	Primer	Sequence (5′-3′)
β-actin	NM_007393	440F	CCAGATCATGTTTGAGACCTTCAA
		526R	GTGGTACGACCAGAGGCATACA
Ryr2	NM_023868	4676F	ACCAAGCCAGATTACAGCACAG
		4899R	ACCGTCACTGTGCGCACTC
NCX	NM_011406	1923F	TCGATGACGAGGAGTATGAGAA
		2031R	CCACCAAGCTCATTCAACAA
ErbB4	NM_010154	431F	AACAGCAGTACCGAGCCTTG
		530R	AAGGAGAGGTCCCGGTTG
Sumo1	NM_009460	803F	TGCTTCACTCCTGGACTGTG
		1003R	TCTCTCCAGTGAAGCCACCT
INSR	NM_010568	1138F	AAAGTTTGCCCAACCATCTG
		1359R	GTGAAGGTCTTGGCAGAAGC
GATA3	NM_00809l	246F	GTGGTCACACTCGGATTCCT
		435R	GCAAAAAGGAGGGTTTAGGG
Cubn	NM_1081084	5921F	GAAGGGGATTCCTTCTGG
		6029R	AGGGGTGTCTCCTGTCAC
Gstp2	NM_181796	190F	AGCCCACTTGTCTGTATGG
		425R	AGGGCCTTCACGTAGTCAT

Table 2

Physical outcomes of Day 10 embryos

Results from gross examination of every embryo removed from the dam are reported. Non-exposed controls (CTL) and 10ppb TCE exposed (TCE) embryos are sub-categorized into 0mg/kg (0CTL and 0TCE), 2mg/kg (2CTL and 2TCE), and 8mg/kg folate (8 CTL and 8TCE) groups. Developmental staging was according to Kaufman, 1992. Reabsorptions indicate empty amniotic sacs and false pregnancy denote no pregnancy development in any way. The amount of embryos are shown on a per litter basis (n) and by the percent of embryos compared to the overall total per treatment group (%).

	control water			10ppb TCE water		
	0mg folate	**2mg folate**	**8mg folate**	**0mg folate**	**2mg folate**	**8mg folate**
viable embryos	130	75	94	102	89	102
litters	22	9	11	17	13	17
False Pregnancy [*n* (%)]	0.18 (3.08)	0.22 (2.67)	0.18 (2.13)	0.24 (3.92)	0.08 (1.12)	0.11 (1.96)
Reabsorptions/Abortions [n (%)]	1.64 (27.69)	1.78 (21.33)	2.27 (26.60)	1.29 (21.33)	1.08 (15.73)	0.94 (16.67)
Under-development [n (%)]	0.77 (13.08)	0.67 (8.0)	0.82 (9.57)	0.35 (5.88)	1.08 (15.73)	0.50 (8.82)
Normal development [n (%)]	3.18 (53.85)	5.67 (68.0)	5.09 (59.57)	4.12 (68.63)	4.54 (66.29)	4.0 (70.59)

n = per litter basis

% = percent of total embryos

Table 3

Calcium pathway

A) Over and B) under expressed genes involved in the calcium signaling pathway. Each column as described in Table 3.

Calcium Pathway									
Over-Expressed									
			1	**2**	**3**	**4**	**5**	**6**	**7**
Sequence ID	**Gene ID**	**Description**	**0 CTL v 0 TCE**	**2 CTL v 2 TCE**	**8 CTL v 8 TCE**	**2 TCE v 0 TCE**	**2 TCE v 8 TCE**	**2 CTL v 0 CTL**	**2 CTL v 8 CTL**
ENSMUST105420	Adora2a	adenosine A2a receptor			■		■		
NM_009781	Cacna1c	calcium channel			■		■		
NM_009783	Cacna1g	calcium channel						■	
ENSMUST31093	Cckar	cholecystokinin A receptor				■			
NM_203491	Chrm2	cholinergic receptor			■				
ENSMUST81091	Erbb4	v-erb-a erythroblastic leukemia viral oncogene homolog 4			■				
ENSMUST106091	Gjb3	gap junction membrane channel protein beta 3			■				■
NM_010305	Gnai1	guanine nucleotide binding protein			■				
NM_008170	Grin2a	glutamate receptor				■		■	
NM_001081414	Grm5	glutamate receptor				■		■	
NM_001012306	Hsd3b3	hydroxy-delta-5-steroid dehydrogenase					■		
NM_010568	Insr	insulin receptor			■		■		
NM_010585	Itpr1	inositol 1			■		■		
NM_019923	Itpr2	inositol 1			■		■		
ENSMUST72460	Mef2a	myocyte enhancer factor 2A			■		■		
NM_011058	Pdgfra	platelet derived growth factor receptor				■	■	■	
NM_008809	Pdgfrb	platelet derived growth factor receptor						■	
NM_001077495	Pik3r1	phosphatidylinositol 3-kinase			■				
NM_013829	Plcb4	phospholipase C			■				
NM_019588	Plce1	phospholipase C			■				
ENSMUST27997	Rgs5	regulator of G-protein signaling 5			■				
NM_023868	Ryr2	ryanodine receptor 2			■		■		
NM_177652	Ryr3	ryanodine receptor 3			■				
ENSMUST57311	Sfn	stratifin				■	■	■	■
NM_011406	Slc8a1	solute carrier family 8 (sodium/calcium exchanger)			■				
NM_001081011	Srgap2	SLIT-ROBO Rho GTPase activating protein 2			■				
NM_018753	Ywhab	tyrosine 3-monooxygenase/tryptophan 5-monooxygenase activation protein			■				

Under-expressed									
			1	**2**	**3**	**4**	**5**	**6**	**7**
Sequence ID	**Gene ID**	**Description**	**0 CTL v 0 TCE**	**2 CTL v 2 TCE**	**8 CTL v 8 TCE**	**2 TCE v 0 TCE**	**2 TCE v 8 TCE**	**2 CTL v 0 CTL**	**2 CTL v 8 CTL**
ENSMUST114913	Adcy5	adenylate cyclase 5					■		
ENSMUST109749	Akt1	thymoma viral proto-oncogene 1					■		
NM_009721	Atp1b1	ATPase				■		■	
NM_213616	Atp2b4	ATPase		■					■
NM_021415	Cacna1h	calcium channel						■	■
ENSMUST32409	Camk1	calcium/calmodulin-dependent protein kinase I				■		■	
ENSMUST29454	Casq2	calsequestrin 2				■		■	■
ENSMUST87104	Cdkl5	cyclin-dependent kinase-like 5							■
NM_203491	Chrm2	cholinergic receptor							■
ENSMUST22718	Ednrb	endothelin receptor type B							■
NM_001003817	Erbb2	v-erb-b2 erythroblastic leukemia viral oncogene homolog 2						■	
ENSMUST81091	Erbb4	v-erb-a erythroblastic leukemia viral oncogene homolog 4						■	■
ENSMUST59193	F2r	coagulation factor II (thrombin) receptor							■
ENSMUST106091	Gjb3	gap junction membrane channel protein beta 3			■				
NM_010305	Gnai1	guanine nucleotide binding protein				■		■	■
NM_008139	Gnaq	guanine nucleotide binding protein				■		■	■
NM_010312	Gnb2	guanine nucleotide binding protein			■				
NM_138719	Gnb5	guanine nucleotide binding protein					■		
NM_025331	Gng11	guanine nucleotide binding protein		■		■	■	■	■
NM_010318	Gng5	guanine nucleotide binding protein				■		■	■
NM_010568	Insr	insulin receptor							■
NM_001081175	Itpkb	inositol 1						■	■
NM_019923	Itpr2	inositol 1							■
NM_010605	Kcnj5	potassium inwardly-rectifying channel				■		■	■
ENSMUST24916	Lhcgr	luteinizing hormone/choriogonadotropin receptor						■	
BC040217	Mef2d	myocyte enhancer factor 2D						■	■
ENSMUST35800	Nfatc1	nuclear factor of activated T-cells		■				■	■
ENSMUST33086	Phkg2	phosphorylase kinase				■			
NM_013829	Plcb4	phospholipase C							■
NM_019676	Plcd1	phospholipase C						■	
NM_019588	Plce1	phospholipase C							■
NM_024459	Ppp3r1	protein phosphatase 3			■		■		
NM_008854	Prkaca	protein kinase						■	
NM_008855	Prkcb1	protein kinase C							■
ENSMUST97275	Prkce	protein kinase C						■	
NM_008856	Prkch	protein kinase C						■	■

Under-expressed									
			1	**2**	**3**	**4**	**5**	**6**	**7**
Sequence ID	**Gene ID**	**Description**	**0 CTL v 0 TCE**	**2 CTL v 2 TCE**	**8 CTL v 8 TCE**	**2 TCE v 0 TCE**	**2 TCE v 8 TCE**	**2 CTL v 0 CTL**	**2 CTL v 8 CTL**
ENSMUST27603	Rgs18	regulator of G-protein signaling 18				■			■
NM_019769	Rik	RIKEN cDNA 1500003O03 gene					■		
NM_023868	Ryr2	ryanodine receptor 2						■	■
NM_011406	Slc8a1	solute carrier family 8 (sodium/calcium exchanger)					■	■	■
ENSMUST9036	Vdac3	voltage-dependent anion channel 3					■	■	■
NM_018753	Ywhab	tyrosine 3-monooxygenase/tryptophan 5-monooxygenase activation protein							■
NM_011739	Ywhaq	tyrosine 3-monooxygenase/tryptophan 5-monooxygenase activation protein				■		■	■

Table 4

Ion channel pathway

A) Over and B) under expressed genes involved in the ion channel signaling pathway. Each column as described in Table 3.

Ion Channel Pathway									
Over-Expressed									
			1	**2**	**3**	**4**	**5**	**6**	**7**
Sequence ID	**Gene ID**	**Description**	**0 CTL v 0 TCE**	**2 CTL v 2 TCE**	**8 CTL v 8 TCE**	**2 TCE v 0 TCE**	**2 TCE v 8 TCE**	**2 CTL v 0 CTL**	**2 CTL v 8 CTL**
NM_009781	Cacna1c	calcium channel	■	■	■	■	■	■	■
NM_009783	Cacna1g	calcium channel			■		■		
NM_009784	Cacna2d1	calcium channel						■	
NM_007582	Cacng1	calcium channel				■			
BC051033	Fxyd3	FXYD domain-containing ion transport regulator 3						■	■
NM_146017	Gabrp	gamma-aminobutyric acid receptor			■	■	■	■	■
ENSMUST76349	Gria3	glutamate receptor						■	
NM_008170	Grin2a	glutamate receptor				■		■	
ENSMUST72602	Hvcn1	hydrogen voltage-gated channel 1						■	
NM_010585	Itpr1	inositol 1			■				
NM_019923	Itpr2	inositol 1			■				
NM_010597	Kcnab1	potassium voltage-gated channel				■		■	
NM_134110	Kcne2	potassium voltage-gated channel			■		■		
NM_020574	Kcne3	potassium voltage-gated channel			■		■		
NM_010603	Kcnj12	potassium inwardly-rectifying channel					■		
ENSMUST46765	Kcnk1	potassium channel			■		■	■	
NM_008431	Kcnk4	potassium channel							■
NM_023872	Kcnq5	potassium voltage-gated channel			■				
NM_173417	Kcns3	potassium voltage-gated channel					■		
ENSMUST39450	Mcoln3	mucolipin 3						■	
NM_023868	Ryr2	ryanodine receptor 2			■		■		
NM_001099298	Scn2a1	sodium channel			■		■		
NM_153417	Trpm6	transient receptor potential cation channel			■		■		
ENSMUST103224	Trpm7	transient receptor potential cation channel			■				
NM_022413	Trpv6	transient receptor potential cation channel			■		■		

Under-expressed									
			1	**2**	**3**	**4**	**5**	**6**	**7**
Sequence ID	**Gene ID**	**Description**	**0 CTL v 0 TCE**	**2 CTL v 2 TCE**	**8 CTL v 8 TCE**	**2 TCE v 0 TCE**	**2 TCE v 8 TCE**	**2 CTL v 0 CTL**	**2 CTL v 8 CTL**
ENSMUST49346	Accn3	amiloride-sensitive cation channel 3		■					
NM_021415	Cacna1h	calcium channel						■	■
NM_009784	Cacna2d1	calcium channel							■
NM_023116	Cacnb2	calcium channel						■	■
NM_001037099	Cacnb4	calcium channel		■					
ENSMUST45706	Cftr	cystic fibrosis transmembrane conductance regulator homolog							■
ENSMUST71697	Fxyd1	FXYD domain-containing ion transport regulator 1							■
BC031112	Fxyd5	FXYD domain-containing ion transport regulator 5		■					
NM_008070	Gabrb2	gamma-aminobutyric acid (GABA-A) receptor						■	■
NM_146017	Gabrp	gamma-aminobutyric acid (GABA-A) receptor	■						
NM_019923	Itpr2	inositol 1							■
NM_145983	Kcna5	potassium voltage-gated channel						■	
NM_008424	Kcne1	potassium voltage-gated channel				■		■	
NM_020574	Kcne3	potassium voltage-gated channel						■	■
NM_010600	Kcnh1	potassium voltage-gated channel		■					
NM_013569	Kcnh2	potassium voltage-gated channel			■				
ENSMUST39366	Kcnh8	potassium voltage-gated channel		■				■	■
NM_145963	Kcnj14	potassium inwardly-rectifying channel	■						
NM_010604	Kcnj16	potassium inwardly-rectifying channel							■
ENSMUST42970	Kcnj2	potassium inwardly-rectifying channel				■		■	■
NM_010605	Kcnj5	potassium inwardly-rectifying channel		■					
NM_001033876	Kcnk9	potassium channel		■					
NM_010610	Kcnma1	potassium large conductance calcium-activated channel		■					■
NM_031169	Kcnmb1	potassium large conductance calcium-activated channel						■	■
NM_080465	Kcnn2	potassium intermediate/small conductance calcium-activated channel						■	■
NM_023872	Kcnq5	potassium voltage-gated channel							■
ENSMUST22272	Kctd6	potassium channel tetramerisation domain containing 6		■				■	■
ENSMUST67951	Kctd9	potassium channel tetramerisation domain containing 9							■
ENSMUST23509	Klhl24	kelch-like 24 (Drosophila							■
ENSMUST39450	Mcoln3	mucolipin 3							■
NM_177755	Rik	RIKEN cDNA 8230402K04 gene				■			

Under-expressed									
			1	**2**	**3**	**4**	**5**	**6**	**7**
Sequence ID	**Gene ID**	**Description**	**0 CTL v 0 TCE**	**2 CTL v 2 TCE**	**8 CTL v 8 TCE**	**2 TCE v 0 TCE**	**2 TCE v 8 TCE**	**2 CTL v 0 CTL**	**2 CTL v 8 CTL**
NM_023868	Ryr2	ryanodine receptor 2							
BC039140	Scn1b	sodium channel							
NM_001099298	Scn2a1	sodium channel							
NM_018732	Scn3a	sodium channel							
NM_013838	Trpc6	transient receptor potential cation channel							
ENSMUST103224	Trpm7	transient receptor potential cation channel							
ENSMUST9036	Vdac3	voltage-dependent anion channel 3							

Table 5

Cell cycle pathway

A) Over and B) under expressed genes involved in the cell cycle pathway. Each column as described in Table 3.

Cell Cycle Pathway									
Over-Expressed									
			1	**2**	**3**	**4**	**5**	**6**	**7**
Sequence ID	**Gene ID**	**Description**	**0 CTL v 0 TCE**	**2 CTL v 2 TCE**	**8 CTL v 8 TCE**	**2 TCE v 0 TCE**	**2 TCE v 8 TCE**	**2 CTL v 0 CTL**	**2 CTL v 8 CTL**
BC028526	Anapc13	anaphase promoting complex subunit 13	■						
ENSMUST79362	Apc	adenomatosis polyposis coli			■				
ENSMUST37440	Atm	ataxia telangiectasia mutated homolog (human)				■			
ENSMUST86248	Aurkc	aurora kinase C				■		■	
ENSMUST74077	Bmp4	bone morphogenetic protein 4			■				
NM_007561	Bmpr2	bone morphogenic protein receptor			■				
ENSMUST107228	Brca1	breast cancer 1			■				
ENSMUST44620	Brca2	breast cancer 2			■				
ENSMUST93517	Casp3	caspase 3				■			
NM_001081062	Ccno	cyclin O							■
BC005775	Cdc26	cell division cycle 26							■
ENSMUST42410	Cdk6	cyclin-dependent kinase 6			■				
ENSMUST22009	Cetn3	centrin 3			■			■	■
ENSMUST75853	Cks2	CDC28 protein kinase regulatory subunit 2				■			■
ENSMUST49404	Clasp1	CLIP associating protein 1			■				
ENSMUST35089	Clasp2	CLIP associating protein 2			■				
ENSMUST6293	Crkl	v-crk sarcoma virus CT10 oncogene homolog (avian)-like		■				■	
ENSMUST5841	Ctcf	CCCTC-binding factor			■				
ENSMUST31697	Cul1	cullin 1			■		■		
ENSMUST26475	Ddit3	DNA-damage inducible transcript 3			■				
AF396877	Dst	dystonin			■		■		
NM_013507	Eif4g2	eukaryotic translation initiation factor 4						■	
ENSMUST81091	Erbb4	v-erb-a erythroblastic leukemia viral oncogene homolog 4 (avian)			■				
BC048734	Fgf8	fibroblast growth factor 8							■
ENSMUST9777	G0s2	G0/G1 switch gene 2							■
ENSMUST43098	Gadd45a	growth arrest and DNA-damage-inducible 45 alpha			■		■		
ENSMUST32129	Gkn1	gastrokine 1				■			
ENSMUST21729	Gpr132	G protein-coupled receptor 132					■		

Cell Cycle Pathway									
Over-Expressed									
			1	**2**	**3**	**4**	**5**	**6**	**7**
Sequence ID	**Gene ID**	**Description**	**0 CTL v 0 TCE**	**2 CTL v 2 TCE**	**8 CTL v 8 TCE**	**2 TCE v 0 TCE**	**2 TCE v 8 TCE**	**2 CTL v 0 CTL**	**2 CTL v 8 CTL**
ENSMUST57884	Gps2	G protein pathway suppressor 2					■		
ENSMUST23507	Gsk3b	glycogen synthase kinase 3 beta			■				
ENSMUST80030	Gspt1	G1 to S phase transition 1		■					
ENSMUST38777	Hipk2	homeodomain interacting protein kinase 2			■				
ENSMUST28882	Il1a	interleukin 1 alpha			■		■		
ENSMUST12587	Kif11	kinesin family member 11						■	
U67204	Macf1	microtubule-actin crosslinking factor 1			■		■		
ENSMUST4986	Mapk13	mitogen activated protein kinase 13					■	■	■
NM_134092	Mtbp	Mdm2			■				
ENSMUST52965	Nipbl	Nipped-B homolog (Drosophila)			■				
NM_010151	Nr2f1	nuclear receptor subfamily 2		■					
ENSMUST78259	Nsl1	NSL1		■				■	■
ENSMUST25204	Pfdn1	prefoldin 1	■						
ENSMUST18361	Pmp22	peripheral myelin protein				■		■	
ENSMUST101534	Ptn	pleiotrophin				■		■	■
ENSMUST49009	Rad9b	RAD9 homolog B (S. cerevisiae)			■				
ENSMUST28814	Rassf2	Ras association (RalGDS/AF-6) domain family 2		■					■
ENSMUST35842	Rassf4	Ras association (RalGDS/AF-6) domain family 4			■				
ENSMUST22701	Rb1	retinoblastoma 1			■				
ENSMUST29170	Rbl1	retinoblastoma-like 1 (p107)			■				
ENSMUST34091	Rbl2	retinoblastoma-like 2			■				
ENSMUST102864	Rel	reticuloendotheliosis oncogene			■				
NM_175238	Rif1	Rap 1 interacting factor 1 homolog (yeast)			■				
ENSMUST73926	Rps12	ribosomal protein S12							■
ENSMUST27495	Sept2	septin 2						■	
ENSMUST23095	Sept3	septin 3						■	
ENSMUST30724	Sesn2	sestrin 2			■		■		
ENSMUST57311	Sfn	stratifin				■	■	■	■
BC086683	Spc24	SPC24							■
NM_001081008	Taf1	TAF1 RNA polymerase II		■				■	
ENSMUST45288	Tgfb2	transforming growth factor		■				■	
NM_172664	Tlk1	tousled-like kinase 1		■				■	
AB020317	Trp53	transformation related protein 53						■	
ENSMUST71648	Vegfa	vascular endothelial growth factor A			■				

Under-expressed									
			1	**2**	**3**	**4**	**5**	**6**	**7**
Sequence ID	**Gene ID**	**Description**	**0 CTL v 0 TCE**	**2 CTL v 2 TCE**	**8 CTL v 8 TCE**	**2 TCE v 0 TCE**	**2 TCE v 8 TCE**	**2 CTL v 0 CTL**	**2 CTL v 8 CTL**
BC028526	Anapc13	anaphase promoting complex subunit 13						■	
ENSMUST25561	Anxa1	annexin A1					■	■	■
NM_009686	Apbb2	amyloid beta (A4) precursor protein-binding							■
ENSMUST29842	Bcl10	B-cell leukemia/lymphoma 10					■		
AF271733	Bin3	bridging integrator 3			■				
ENSMUST28836	Bmp2	bone morphogenetic protein 2				■	■	■	■
NM_007561	Bmpr2	bone morphogenic protein receptor							■
BC061001	Bmyc	brain expressed myelocytomatosis oncogene						■	
NM_009770	Btg3	B-cell translocation gene 3						■	
NM_021550	C1galt1c1	C1GALT1-specific chaperone 1						■	■
BC052789	Cables2	Cdk5 and Abl enzyme substrate 2				■	■		
ENSMUST93517	Casp3	caspase 3			■				
ENSMUST48192	Ccdc5	coiled-coil domain containing 5			■				
BC085238	Ccnb1	cyclin B1					■		
BC060180	Ccng2	cyclin G2							■
ENSMUST114077	Ccnyl1	cyclin Y-like 1				■			
BC005775	Cdc26	cell division cycle 26			■				
ENSMUST50148	Cdc37l1	cell division cycle 37 homolog (S. cerevisiae)-like 1							■
BC003893	Cdc5l	cell division cycle 5-like (S. pombe)				■			■
ENSMUST42410	Cdk6	cyclin-dependent kinase 6							■
ENSMUST23829	Cdkn1a	cyclin-dependent kinase inhibitor 1A (P21)		■					■
ENSMUST3115	Cdkn1b	cyclin-dependent kinase inhibitor 1B				■	■	■	■
BC049694	Cdkn3	cyclin-dependent kinase inhibitor 3			■				
ENSMUST22009	Cetn3	centrin 3			■				
ENSMUST68532	Cgrrf1	cell growth regulator with ring finger domain 1						■	■
ENSMUST29679	Cks1b	CDC28 protein kinase 1b				■		■	■
ENSMUST75853	Cks2	CDC28 protein kinase regulatory subunit 2			■				
ENSMUST27050	Cops5	COP9 (constitutive photomorphogenic) homolog			■	■	■	■	■
ENSMUST17920	Crk	v-crk sarcoma virus CT10 oncogene homolog (avian)							■
ENSMUST4478	Cul3	cullin 3							■
NM_027545	Cwf19l2	CWF19-like 2							■
ENSMUST103129	Dsn1	DSN1				■		■	
ENSMUST103145	E2f1	E2F transcription factor 1						■	

Under-expressed									
			1	**2**	**3**	**4**	**5**	**6**	**7**
Sequence ID	**Gene ID**	**Description**	**0 CTL v 0 TCE**	**2 CTL v 2 TCE**	**8 CTL v 8 TCE**	**2 TCE v 0 TCE**	**2 TCE v 8 TCE**	**2 CTL v 0 CTL**	**2 CTL v 8 CTL**
AY957576	E2f8	E2F transcription factor 8							■
ENSMUST1757	Eef1e1	eukaryotic translation elongation factor 1 epsilon 1				■		■	
NM_001003817	Erbb2	v-erb-b2 erythroblastic leukemia viral oncogene homolog 2						■	■
ENSMUST81091	Erbb4	v-erb-a erythroblastic leukemia viral oncogene homolog 4 (avian)						■	■
NM_007951	Erh	enhancer of rudimentary homolog (Drosophila)			■			■	
NM_011809	Ets2	E26 avian leukemia oncogene 2						■	
ENSMUST81028	Etv6	ets variant gene 6 (TEL oncogene)				■			
NM_001033244	Fancd2	Fanconi anemia							■
ENSMUST19907	Fbxo5	F-box protein 5				■	■	■	■
ENSMUST187	Fgf6	fibroblast growth factor 6			■				■
ENSMUST62292	Foxc1	forkhead box C1							■
ENSMUST15456	Gadd45b	growth arrest and DNA-damage-inducible 45 beta			■			■	
ENSMUST32129	Gkn1	gastrokine 1		■					
NM_008179	Gspt2	G1 to S phase transition 2						■	■
ENSMUST34026	Hpgd	hydroxyprostaglandin dehydrogenase 15 (NAD)					■		■
BC024581	Hrasls3	HRAS like suppressor 3			■				
ENSMUST65537	Jmy	junction-mediating and regulatory protein						■	■
ENSMUST103032	Llgl2	lethal giant larvae homolog 2 (Drosophila)						■	■
NM_010755	Maff	v-maf musculoaponeurotic fibrosarcoma oncogene family						■	■
ENSMUST25078	Map3k8	mitogen activated protein kinase kinase kinase 8						■	■
ENSMUST88827	Mapk12	mitogen-activated protein kinase 12						■	■
ENSMUST57669	Mapk3	mitogen activated protein kinase 3			■		■		
NM_133350	Mapre3	microtubule-associated protein						■	
ENSMUST34303	Mphosph6	M phase phosphoprotein 6						■	
NM_134092	Mtbp	Mdm2							■
ENSMUST22971	Myc	myelocytomatosis oncogene							■
NM_144931	Nae1	NEDD8 activating enzyme E1 subunit 1			■	■	■		
NM_133762	Ncapg2	non-SMC condensin II complex							■
ENSMUST35800	Nfatc1	nuclear factor of activated T-cells		■				■	■
NM_010151	Nr2f1	nuclear receptor subfamily 2				■			
NM_001024622	Pcnp	PEST proteolytic signal containing nuclear protein					■		
ENSMUST25204	Pfdn1	prefoldin 1						■	

Under-expressed									
			1	**2**	**3**	**4**	**5**	**6**	**7**
Sequence ID	**Gene ID**	**Description**	**0 CTL v 0 TCE**	**2 CTL v 2 TCE**	**8 CTL v 8 TCE**	**2 TCE v 0 TCE**	**2 TCE v 8 TCE**	**2 CTL v 0 CTL**	**2 CTL v 8 CTL**
ENSMUST36374	Phb	prohibitin			■				
ENSMUST34689	Pin1	protein (peptidyl-prolyl cis/trans isomerase) NIMA-interacting 1			■				
ENSMUST56370	Pmf1	polyamine-modulated factor 1			■				
NM_198600	Pols	polymerase (DNA directed) sigma						■	
NM_008014	Ppm1g	protein phosphatase 1G (formerly 2C)			■				
NM_024209	Ppp6c	protein phosphatase 6					■		
ENSMUST20685	Pttg1	pituitary tumor-transforming 1					■	■	■
ENSMUST22136	Rad17	RAD17 homolog (S. pombe)							■
ENSMUST20649	Rad50	RAD50 homolog (S. cerevisiae)							■
ENSMUST90678	Rap1a	RAS-related protein-1a					■		
ENSMUST22701	Rb1	retinoblastoma 1							■
ENSMUST27040	Rb1cc1	RB1-inducible coiled-coil 1			■			■	
ENSMUST102598	Rbbp4	retinoblastoma binding protein 4				■			
ENSMUST34091	Rbl2	retinoblastoma-like 2							■
BC051473	Rbx1	ring-box 1			■			■	
ENSMUST84250	Rcc1	regulator of chromosome condensation 1			■			■	
NM_007483	Rhob	ras homolog gene family				■		■	
NM_028228	Rik	RIKEN cDNA 2610028A01 gene			■				
ENSMUST73926	Rps12	ribosomal protein S12			■		■		
NM_009101	Rras	Harvey rat sarcoma oncogene			■		■		
BC010774	S100a6	S100 calcium binding protein A6 (calcyclin)			■				
ENSMUST23457	Senp5	SUMO/sentrin specific peptidase 5							■
ENSMUST30724	Sesn2	sestrin 2						■	
BC086683	Spc24	SPC24				■	■		
NM_001005370	Spin2	spindlin family							■
ENSMUST29448	Sycp1	synaptonemal complex protein 1				■	■		
ENSMUST11258	Tbrg1	transforming growth factor beta regulated gene 1						■	
ENSMUST2678	Tgfb1	transforming growth factor							■
ENSMUST39562	Trim13	tripartite motif protein 13				■	■	■	■
NM_021884	Tsg101	tumor susceptibility gene 101						■	■
ENSMUST25914	Vegfb	vascular endothelial growth factor B						■	■
ENSMUST21985	Zfp369	zinc finger protein 369							■

Table 6

Apoptosis pathway

A) Over and B) under expressed genes involved in the apoptosis pathway. Each column as described in Table 3.

Apoptosis Pathway									
Over-expressed									
			1	**2**	**3**	**4**	**5**	**6**	**7**
Sequence ID	**Gene ID**	**Description**	**0 CTL v 0 TCE**	**2 CTL v 2 TCE**	**8 CTL v 8 TCE**	**2 TCE v 0 TCE**	**2 TCE v 8 TCE**	**2 CTL v 0 CTL**	**2 CTL v 8 CTL**
ENSMUST103020	Aatk	apoptosis-associated tyrosine kinase						■	■
NM 007536	Bcl2a1d	B-cell leukemia/lymphoma 2 related protein A1d				■	■		
ENSMUST115094	Birc4	baculoviral IAP repeat-containing 4			■				
ENSMUST107228	Brca1	breast cancer 1			■				
ENSMUST31895	Casp2	caspase 2						■	
ENSMUST93517	Casp3	caspase 3				■			
NM 001042605	Cd74	CD74 antigen (invariant polypeptide of major histocompatibility complex			■		■		
ENSMUST46506	Clcf1	cardiotrophin-like cytokine factor 1							■
ENSMUST53594	Cradd	CASP2 and RIPK1 domain containing adaptor with death domain						■	
ENSMUST31697	Cul1	cullin 1			■				
BC092213	Cycs	cytochrome c		■					
ENSMUST26475	Ddit3	DNA-damage inducible transcript 3			■		■		
ENSMUST37907	Ddx58	DEAD (Asp-Glu-Ala-Asp) box polypeptide 58			■		■		
ENSMUST84488	Dock1	dedicator of cyto-kinesis 1			■				
ENSMUST39516	Egln3	EGL nine homolog 3 (C. elegans)			■				
ENSMUST27066	Eya1	eyes absent 1 homolog (Drosophila)		■	■			■	■
ENSMUST25691	Fas	Fas (TNF receptor superfamily member 6)				■			
NM 010185	Fcer1g	Fc receptor			■		■		
BC048734	Fgf8	fibroblast growth factor 8							■
ENSMUST57884	Gps2	G protein pathway suppressor 2					■		
ENSMUST23507	Gsk3b	glycogen synthase kinase 3 beta			■				
ENSMUST30683	Hgf	hepatocyte growth factor		■				■	■
ENSMUST38777	Hipk2	homeodomain interacting protein kinase 2			■				
NM 010478	Hspa1b	heat shock protein 1B	■						
NM 010414	Htt	huntingtin			■				
ENSMUST20702	Igfbp3	insulin-like growth factor binding protein 3			■		■		
ENSMUST102786	Itgb3bp	integrin beta 3 binding protein (beta3-endonexin)		■					

Apoptosis Pathway

Over-expressed

			1	2	3	4	5	6	7
Sequence ID	**Gene ID**	**Description**	**0 CTL v 0 TCE**	**2 CTL v 2 TCE**	**8 CTL v 8 TCE**	**2 TCE v 0 TCE**	**2 TCE v 8 TCE**	**2 CTL v 0 CTL**	**2 CTL v 8 CTL**
ENSMUST49248	Malt1	mucosa associated lymphoid tissue lymphoma translocation gene 1			■				
ENSMUST95806	Map3k5	mitogen activated protein kinase kinase kinase 5			■				
ENSMUST67429	Mdm4	transformed mouse 3T3 cell double minute 4			■				
AK018196	Mitf	microphthalmia-associated transcription factor			■				
ENSMUST28288	Notch1	Notch gene homolog 1 (Drosophila)					■		
ENSMUST30154	Nudt2	nudix (nucleoside diphosphate linked moiety X)-type motif 2	■						
ENSMUST51209	Peg3	paternally expressed 3						■	
ENSMUST32573	Pglyrp1	peptidoglycan recognition protein 1			■		■		
NM 001077495	Pik3r1	phosphatidylinositol 3-kinase			■				
NM 011159	Prkdc	protein kinase			■		■		
AK083198	Prlr	prolactin receptor			■				
ENSMUST59507	Purb	purine rich element binding protein B			■				
ENSMUST6851	Qrich1	glutamine-rich 1			■				
ENSMUST22034	Rasa1	RAS p21 protein activator 1			■				
NM 011279	Rnf7	ring finger protein 7		■					
ENSMUST115866	Rock1	Rho-associated coiled-coil containing protein kinase 1			■				
ENSMUST102843	Rtn4	reticulon 4			■				
ENSMUST101118	Rybp	RING1 and YY1 binding protein					■		
NM 001099298	Scn2a1	sodium channel			■		■		
ENSMUST21728	Siva1	SIVA1	■						
NM 011434	Sod1	superoxide dismutase 1					■		
ENSMUST49931	Spn	sialophorin					■		
ENSMUST112747	Spp1	secreted phosphoprotein 1			■		■		
XM 915205	Syngap1	synaptic Ras GTPase activating protein 1 homolog	■				■		
ENSMUST45288	Tgfb2	transforming growth factor			■				
ENSMUST95753	Tia1	cytotoxic granule-associated RNA binding protein 1						■	
NM 178931	Tnfrsf14	tumor necrosis factor receptor superfamily						■	
NM 026654	Toe1	target of EGR1						■	
AF357400	Tpt1	tumor protein						■	
ENSMUST40312	Trib3	tribbles homolog 3 (Drosophila)			■				
AB020317	Trp53	transformation related protein 53						■	

Apoptosis Pathway

Over-expressed

			1	2	3	4	5	6	7
Sequence ID	**Gene ID**	**Description**	**0 CTL v 0 TCE**	**2 CTL v 2 TCE**	**8 CTL v 8 TCE**	**2 TCE v 0 TCE**	**2 TCE v 8 TCE**	**2 CTL v 0 CTL**	**2 CTL v 8 CTL**
ENSMUST40231	Trp63	transformation related protein 63							■
ENSMUST106236	Unc5c	unc-5 homolog C (C. elegans)			■				
ENSMUST71648	Vegfa	vascular endothelial growth factor A			■				
ENSMUST21937	Zfp346	zinc finger protein 346						■	

Under-expressed

			1	2	3	4	5	6	7
Sequence ID	**Gene ID**	**Description**	**0 CTL v 0 TCE**	**2 CTL v 2 TCE**	**8 CTL v 8 TCE**	**2 TCE v 0 TCE**	**2 TCE v 8 TCE**	**2 CTL v 0 CTL**	**2 CTL v 8 CTL**
NM 001033369	Acvr1c	activin A receptor							■
ENSMUST109749	Akt1	thymoma viral proto-oncogene 1						■	
NM 013467	Aldh1a1	aldehyde dehydrogenase family 1							■
ENSMUST329	Alox12	arachidonate 12-lipoxygenase					■	■	■
NM 009686	Apbb2	amyloid beta (A4) precursor protein-binding							■
ENSMUST6828	Aplp1	amyloid beta (A4) precursor-like protein 1					■		■
ENSMUST3066	Apoe	apolipoprotein E			■				
ENSMUST96119	Asah2	N-acylsphingosine amidohydrolase 2		■				■	■
NM 022305	B4galt1	UDP-Gal:betaGlcNAc beta 1							■
ENSMUST108089	Bag1	Bcl2-associated athanogene 1				■	■	■	
ENSMUST54636	Bag5	BCL2-associated athanogene 5							■
ENSMUST33093	Bax	Bcl2-associated X protein						■	
ENSMUST2091	Bcap31	B-cell receptor-associated protein 31			■				
ENSMUST29842	Bcl10	B-cell leukemia/lymphoma 10					■		
ENSMUST66460	Bcl2a1c	B-cell leukemia/lymphoma 2 related protein A1c				■			
ENSMUST22806	Bcl2l2	Bcl2-like 2						■	
ENSMUST115094	Birc4	baculoviral IAP repeat-containing 4							■
NM 172149	Bnip1	BCL2/adenovirus E1B interacting protein 1						■	■
NM 009760	Bnip3	BCL2/adenovirus E1B interacting protein 1						■	■
ENSMUST27499	Bok	Bcl-2-related ovarian killer protein			■				
NM 175362	Card11	caspase recruitment domain family			■				
ENSMUST93517	Casp3	caspase 3			■				
ENSMUST29626	Casp6	caspase 6			■				
ENSMUST26062	Casp7	caspase 7			■		■	■	■
BC055070	Ccl2	chemokine (C-C motif) ligand 2						■	

Under-expressed									
			1	**2**	**3**	**4**	**5**	**6**	**7**
Sequence ID	**Gene ID**	**Description**	**0 CTL v 0 TCE**	**2 CTL v 2 TCE**	**8 CTL v 8 TCE**	**2 TCE v 0 TCE**	**2 TCE v 8 TCE**	**2 CTL v 0 CTL**	**2 CTL v 8 CTL**
NM 001042605	Cd74	CD74 antigen (invariant polypeptide of major histocompatibility complex		■				■	
ENSMUST23829	Cdkn1a	cyclin-dependent kinase inhibitor 1A (P21)		■					■
NM 009883	Cebpb	CCAAT/enhancer binding protein					■	■	
ENSMUST34233	Ciapin1	cytokine induced apoptosis inhibitor 1			■				
NM 007702	Cidea	cell death-inducing DNA fragmentation factor			■				
ENSMUST59091	Clca1	chloride channel calcium activated 1	■			■		■	■
NM 025680	Ctnnbl1	catenin			■				
BC092213	Cycs	cytochrome c			■	■			
ENSMUST111530	Dad1	defender against cell death 1			■				
NM 022994	Dap3	death associated protein 3						■	■
ENSMUST37907	Ddx58	DEAD (Asp-Glu-Ala-Asp) box polypeptide 58		■					
BC024780	Diablo	diablo homolog (Drosophila)			■	■	■		
ENSMUST103145	E2f1	E2F transcription factor 1						■	
ENSMUST55990	Eef1a2	eukaryotic translation elongation factor 1 alpha 2						■	
ENSMUST1757	Eef1e1	eukaryotic translation elongation factor 1 epsilon 1				■		■	
ENSMUST39516	Egln3	EGL nine homolog 3 (C. elegans)				■		■	■
ENSMUST27066	Eya1	eyes absent 1 homolog (Drosophila)	■						
ENSMUST33394	Fadd	Fas (TNFRSF6)-associated via death domain			■				
ENSMUST35038	Faim	Fas apoptotic inhibitory molecule				■		■	
ENSMUST25691	Fas	Fas (TNF receptor superfamily member 6)		■					
ENSMUST73152	Fastkd1	FAST kinase domains 1				■		■	■
ENSMUST27103	Fastkd2	FAST kinase domains 2						■	■
ENSMUST19198	Fis1	fission 1 (mitochondrial outer membrane) homolog (yeast)			■				
ENSMUST75491	Fkbp8	FK506 binding protein 8			■		■		
ENSMUST15456	Gadd45b	growth arrest and DNA-damage-inducible 45 beta			■			■	
NM 010295	Gclc	glutamate-cysteine ligase	■						■
NM 008129	Gclm	glutamate-cysteine ligase					■		
AK005055	Glo1	glyoxalase 1				■	■	■	
ENSMUST82429	Gpx1	glutathione peroxidase 1			■				
XM_001478151	Hbxip	hepatitis B virus × interacting protein			■				
ENSMUST28600	Hipk3	homeodomain interacting protein kinase 3		■					■
ENSMUST26572	Hras1	Harvey rat sarcoma virus oncogene 1						■	
NM 010478	Hspa1b	heat shock protein 1B						■	

Under-expressed									
			1	**2**	**3**	**4**	**5**	**6**	**7**
Sequence ID	**Gene ID**	**Description**	**0 CTL v 0 TCE**	**2 CTL v 2 TCE**	**8 CTL v 8 TCE**	**2 TCE v 0 TCE**	**2 TCE v 8 TCE**	**2 CTL v 0 CTL**	**2 CTL v 8 CTL**
ENSMUST89645	Htra2	HtrA serine peptidase 2						■	
ENSMUST20702	Igfbp3	insulin-like growth factor binding protein 3			■		■	■	■
ENSMUST889	Il4	interleukin 4						■	
ENSMUST102786	Itgb3bp	integrin beta 3 binding protein (beta3-endonexin)				■	■		
ENSMUST47616	Jmjd6	jumonji domain containing 6						■	
ENSMUST65537	Jmy	junction-mediating and regulatory protein						■	■
NM 023788	Mageh1	melanoma antigen							■
AK018196	Mitf	microphthalmia-associated transcription factor				■		■	■
ENSMUST22971	Myc	myelocytomatosis oncogene							■
NM 144931	Nae1	NEDD8 activating enzyme E1 subunit 1			■	■	■		
NM 023312	Ndufa13	NADH dehydrogenase (ubiquinone) 1 alpha subcomplex			■				
ENSMUST5647	Ndufs3	NADH dehydrogenase (ubiquinone) Fe-S protein 3			■			■	
NM 010910	Nefl	neurofilament						■	
ENSMUST53540	Ngfrap1	nerve growth factor receptor (TNFRSF16) associated protein 1			■	■	■	■	
ENSMUST28288	Notch1	Notch gene homolog 1 (Drosophila)		■				■	
ENSMUST23779	Nr4a1	nuclear receptor subfamily 4						■	
ENSMUST21284	Ntn1	netrin 1						■	
NM 028778	Nuak2	NUAK family		■					
ENSMUST30154	Nudt2	nudix (nucleoside diphosphate linked moiety X)-type motif 2				■		■	
ENSMUST57195	Nup62	nucleoporin 62						■	
NM 001081170	Pacs2	phosphofurin acidic cluster sorting protein 2						■	
ENSMUST29424	Pdcd10	programmed cell death 10					■		
ENSMUST32577	Pdcd5	programmed cell death 5			■			■	
ENSMUST22060	Pdcd6	programmed cell death 6			■			■	
ENSMUST27247	Pdcl3	phosducin-like 3						■	
NM 022032	Perp	PERP						■	■
NM 009344	Phlda1	pleckstrin homology-like domain						■	
ENSMUST34296	Pik3r2	phosphatidylinositol 3-kinase			■				
ENSMUST98513	Plekhf1	pleckstrin homology domain containing				■	■	■	■
ENSMUST14578	Plg	plasminogen	■						
ENSMUST33938	Polb	polymerase (DNA directed)						■	
ENSMUST27373	Ppm1f	protein phosphatase 1F (PP2C domain containing)							■
NM 001010836	Ppp1r13l	protein phosphatase 1				■		■	

Under-expressed									
			1	**2**	**3**	**4**	**5**	**6**	**7**
Sequence ID	**Gene ID**	**Description**	**0 CTL v 0 TCE**	**2 CTL v 2 TCE**	**8 CTL v 8 TCE**	**2 TCE v 0 TCE**	**2 TCE v 8 TCE**	**2 CTL v 0 CTL**	**2 CTL v 8 CTL**
BC002034	Prdx2	peroxiredoxin 2			■				
NM 011159	Prkdc	protein kinase							■
NM 011871	Prkra	protein kinase				■			■
ENSMUST59507	Purb	purine rich element binding protein B							■
ENSMUST27040	Rb1cc1	RB1-inducible coiled-coil 1							■
NM 007483	Rhob	ras homolog gene family				■		■	
NM 026443	Rik	RIKEN cDNA 1700020C11 gene			■				
BC051541	Rik	RIKEN cDNA 2600009E05 gene						■	
BC025611	Ripk2	receptor (TNFRSF)-interacting serine-threonine kinase 2							■
NM 019955	Ripk3	receptor-interacting serine-threonine kinase 3			■			■	
AK220529	Rnf130	ring finger protein 130						■	■
NM 011279	Rnf7	ring finger protein 7			■	■	■		
ENSMUST30399	Rragc	Ras-related GTP binding C							■
ENSMUST101118	Rybp	RING1 and YY1 binding protein		■					
ENSMUST78481	Scin	scinderin						■	■
NM 001099298	Scn2a1	sodium channel		■				■	■
ENSMUST21728	Siva1	SIVA1			■			■	
NM 026404	Slc35a4	solute carrier family 35			■			■	
ENSMUST25997	Smndc1	survival motor neuron domain containing 1				■			■
ENSMUST56150	Snrk	SNF related kinase						■	■
ENSMUST102774	Sqstm1	sequestosome 1			■				
ENSMUST27263	Stk17b	serine/threonine kinase 17b (apoptosis-inducing)						■	■
ENSMUST88585	Sulf1	sulfatase 1							■
XM 915205	Syngap 1	synaptic Ras GTPase activating protein 1 homolog (rat)		■				■	■
ENSMUST18407	Tbx5	T-box 5				■			■
NM 025780	Thap2	THAP domain containing				■			
NM 153552	Thoc1	THO complex 1							■
ENSMUST102793	Tm2d1	TM2 domain containing 1					■		■
ENSMUST19997	Tnfaip3	tumor necrosis factor						■	
NM 134131	Tnfaip8	tumor necrosis factor				■		■	■
NM 011609	Tnfrsf1a	tumor necrosis factor receptor superfamily			■				
NM 026654	Toe1	target of EGR1			■				
ENSMUST21471	Txndc1	thioredoxin domain containing 1	■						
ENSMUST50183	Uaca	uveal autoantigen with coiled-coil domains and ankyrin repeats						■	■